

Fotini Katopodes Chow* and Robert L. Street

Environmental Fluid Mechanics Laboratory
Stanford University, Stanford, California

1. INTRODUCTION

Experience with models and schemes for representing the effects of the unresolved motions in large-eddy simulations (LES) suggests that the near-wall and main flow domains require quite different treatments. Virtually all schemes make some special provisions for the near-wall representations. This is especially important when modeling field-scale flows, as the limited grid resolution throughout the domain places extra importance on the quality of the turbulence closure scheme.

A well-known problem in LES is the lack of agreement with logarithmic theory in the near-wall region. The goal of this work was to learn what logical steps and procedures are required for subfilter-scale (SFS) modeling to bring the simulated flow fields into agreement with theoretical expectations in the near-wall region. We examined a specific test case: the neutral, rotation-influenced, rough-wall, field-scale boundary-layer flow considered by Andren *et al.* (1994). A standard atmospheric mesoscale simulation code is used, namely, the Advanced Regional Prediction System (ARPS). Because this is a finite volume LES code for irregular terrain, spectral methods and sharp Fourier cutoffs in filters are not viable options. The only major modifications to the code are those associated with the new subfilter-scale models we have implemented.

The closure model implemented includes the series-expansion subfilter-scale turbulence model of Katopodes *et al.* (2000a,b). *A priori* tests for stratified homogeneous shear flow showed that the series model is superior to eddy viscosity models, as the series model has significantly improved correlations and ratios when compared to DNS values. However, when applied to this rough-wall boundary layer flow simulation, the series model requires augmentation. To better represent the near-wall region, we have adopted a hybrid approach. The series and Smagorinsky models are used in conjunction with the near-wall canopy stress term of Brown *et al.* (2001). Neutral boundary layer simulation tests show significantly improved results: the logarithmic velocity layer near the lower boundary is more closely reproduced, as compared to results with standard closure models.

In this paper, we present the framework for construction of a hybrid, or mixed, LES closure model. We then describe the implementation of this model and results from LES simulations of the neutral boundary layer, and close with a summary.

2. SFS AND SGS MOTIONS

ARPS employs spatially filtered compressible nonhydrostatic Navier-Stokes equations. For this paper, ARPS was operated in an incompressible mode (Xu *et al.* 1996).

*Corresponding author address: Environmental Fluid Mechanics Laboratory, Stanford, CA 94305-4020, email: katopod@stanford.edu

Using Favre filtering to separate the density from the velocity, we define the SFS stress as

$$\tau_{ij} = \overline{u_i u_j} - \overline{u_i} \overline{u_j}, \quad (1)$$

where $\overline{u_i}$ are the filtered velocity components. The filtered equations are not closed due to the nonlinear term $\overline{u_i u_j}$ included in τ_{ij} .

To facilitate our understanding of this stress tensor and to improve turbulence models in the near wall region, it is useful to consider velocity partitioning schemes such as those of Carati *et al.* (2001), Zhou *et al.* (2001), and Hughes *et al.* (2001), and the spectral analysis of van Dijk and Duynkerke (2002). Figure 1 shows a schematic of a typical energy spectrum from a turbulent flow. The spectrum can be separated into three parts. The low wavenumber portion is well-resolved on the grid, and is contained in the velocity \overline{u} . The middle portion represents subfilter-scale motions that are between the filter and grid cutoffs. The last portion on the right contains subgrid-scale motions that cannot be resolved on the grid.

Following Carati *et al.* (2001), this velocity partitioning results in a decomposition for the LES stress tensor $\tau_{ij} = \tau_{A,ij} + \tau_{B,ij}$. The subgrid-scale (SGS) stress portion $\tau_{A,ij}$ depends on scales beyond the resolution domain of the LES, while the filtered-scale stress portion $\tau_{B,ij}$ depends on the differences between the exact and filtered velocity fields within the resolution domain, which we call subfilter-scale motions. This partitioning requires that the filter width be larger than the grid spacing. Note that in a continuous domain, $\tau_{A,ij}$ is zero, since there would be no contribution from subgrid-scale effects. The subfilter-scale component, $\tau_{B,ij}$, can theoretically be computed and does not need to be modeled; an infinite expansion in a series model for $\tau_{B,ij}$ would give the exact solution in this case. In a discrete domain, the contribution of τ_{ij} , and thus $\tau_{A,ij}$, increases with decreasing grid resolution. Near the wall, the $\tau_{A,ij}$ terms become increasingly important.

3. CLOSURE MODELS

Using this framework for the turbulence closure, we can construct models for each component separately. For $\tau_{A,ij}$, we have examined, among others, multi-scale Smagorinsky models (Hughes *et al.* 2001) and the effect of the 4th-order numerical smoothing employed in ARPS to remove high-frequency noise and aliasing (which was not found to be significant). The small-scale Smagorinsky model was limited by discretization errors in the large scale flow we are considering, and did not perform well. Therefore, to model the unclosed term, $\tau_{A,ij}$, a simple gradient diffusion form is assumed:

$$\tau_{A,ij} = -2\nu_T \overline{S}_{ij}, \quad (2)$$

where ν_T is the eddy viscosity, and \overline{S}_{ij} is the resolved strain rate tensor. Despite the known shortcomings of this model, it is convenient to use when energy transfer to the

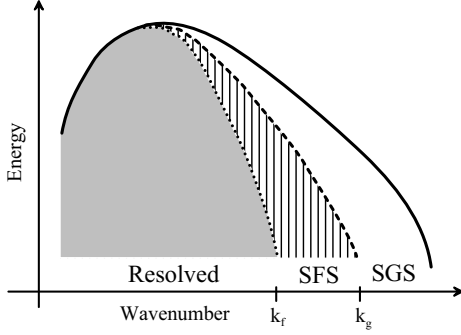


Figure 1: Schematic of velocity energy spectrum showing partitioning into resolved, subfilter-scale, and subgrid-scale motions. The grid and filter cutoff lines are shown as a smooth filter function.

subgrid scales is desired. A common treatment in LES is to use the Smagorinsky model (1963), which assumes

$$\nu_T = (C_S \Delta_g)^2 (2\overline{S_{ij}}\overline{S_{ij}})^{1/2}, \quad (3)$$

where C_S is the Smagorinsky coefficient, and Δ_g is the grid spacing. Such gradient diffusion models are often applied to represent the entire stress tensor τ_{ij} , whereas here we apply the Smagorinsky model as part of a mixed model, so its contribution will not be as pronounced (see Zang *et al.* 1993).

For the stress term $\tau_{B,ij}$, which can be expressed in terms of the resolved velocity, we have implemented the series model of Katopodes *et al.* (2000a), a task for which it is ideally suited. In the spirit of velocity estimation models (Geurts 1997, Domaradzki and Saiki 1997, Stolz and Adams 1999), the series model seeks to obtain an approximate expression for the unresolved variables and use these to calculate the SFS motions. This model uses successive inversion of a Taylor series expansion to express the unfiltered velocity in terms of the filtered (resolved) velocity. We then derive SFS models of arbitrary order of accuracy in the filter width, Δ_f , shown here to fourth order:

$$\begin{aligned} \tau_{ij} = & \overline{\overline{u_i u_j}} - \overline{\overline{u_i}} \overline{\overline{u_j}} - \frac{\Delta_f^2}{24} \overline{\overline{u_i \nabla^2 \overline{u_j}}} - \frac{\Delta_f^2}{24} \overline{\overline{u_j \nabla^2 \overline{u_i}}} \\ & + \frac{\Delta_f^2}{24} \overline{\overline{u_i \nabla^2 \overline{u_j}}} + \frac{\Delta_f^2}{24} \overline{\overline{u_j \nabla^2 \overline{u_i}}}. \end{aligned} \quad (4)$$

The first two terms are analogous to the Leonard terms in the SFS stress; the higher order derivative terms can be shown to be dissipative (Clark *et al.* 1977). An anisotropic Gaussian filter is used, though an isotropic filter Δ_f is shown here for simplicity (see Katopodes *et al.* (2000a) for further details). Other spatially compact filters give similar results, with a change in the expansion coefficients. It is important that the filter width be at least twice the size of the grid spacing, otherwise discretization errors will be as large as the effect of the SFS model (Ghosal 1996, Chow and Moin 2002). The series models also satisfy the full evolution equation for τ_{ij} meaning that the effects of buoyancy, Coriolis forcing, pressure, and advection are naturally included in the model and do not need special treatment (Katopodes *et al.* 2000a).

This series model can be rewritten as

$$\tau_{ij} = \frac{\Delta_f^2}{12} \frac{\partial \overline{u_i}}{\partial x_m} \frac{\partial \overline{u_j}}{\partial x_m}, \quad (5)$$

which is equivalent to equation (4) to the fourth order in the filter width (Katopodes *et al.* 2000a). Equation 4 is similar to the model proposed by Clark *et al.* (1977). This modified Clark model is considerably simpler than equation (4) to implement numerically, so we adopt this as our model for $\tau_{B,ij}$. This model has been used in a channel flow by Fischer and Iliescu (2001) to represent the entire turbulence term with good results. Winkelmann *et al.* (2001) performed a channel flow simulation using the modified Clark model together with the Smagorinsky model, as we do. However, both of these studies considered small-scale flow cases where viscous motions could be resolved near the wall, which is not possible in the atmospheric boundary layer. Vreman *et al.* (1996) also found that a mixed model with the original Clark model performed well for a small-scale temporal mixing layer.

Because of the resolution limitations present when simulating a field-scale flow, the turbulence model requires special treatment near the lower boundary which is rough. This mixed model using equations (2,3) and (5) has limitations near the solid lower boundary, where eddy sizes decrease much more rapidly than the grid spacing. Because the vertical grid-spacings are invariably smaller than the horizontal ones, $2 * dx$ is the minimum vertical distance from the wall for eddies of the horizontal grid size to be resolved. This lack of resolution means that an additional stress term may be needed near the wall to represent these motions. Thus, in this near-wall region, such augmentation of the stress models is appropriate. Following Brown *et al.* (2001) and Cederwall and Street (2002), we implement a canopy stress model near the wall.

The canopy model can be expressed as a forcing term in the horizontal momentum equations as $-C_c a(z) |\overline{u}| \overline{u_i}$ where $i = 1, 2$. Here C_c is a scaling factor and $a(z)$ is a constant smoothing function which are both predetermined. Following Brown *et al.* (2001), we choose $a = \cos^2(\pi z / 2h_c)$ for $z < h_c$, where h_c is the canopy height. Above the canopy, we set $a = 0$. This function $a(z)$ allows for a smooth decay of the forcing canopy function as the specified canopy height is approached.

In the code, the canopy force is treated as part of the turbulence closure stress term, and therefore is integrated numerically using the trapezoidal rule from

$$\tau_{i,can} = - \int C_c a(z) |\overline{u}| \overline{u_i} dz, \quad (6)$$

where the integration constants are chosen so that $\tau_{i,can} = 0$ at the top of the canopy. This stress is then directly added to the τ_{i3} terms contributed from the other model components. Brown *et al.* (2001) choose a constant value for C_c so that the velocity at the top of the canopy matches that from experimental measurements. Cederwall (2001) selected C_c such that the canopy model augmented the total stress at the first grid point above the wall to make it equal to the local bottom shear stress. Instead we allow C_c to be locally proportional to the bottom shear stress in each horizontal direction. The proportionality factor is chosen to allow the canopy to provide the necessary augmentation that will yield logarithmic mean velocity profiles near the wall.

4. NEUTRAL BOUNDARY LAYER SIMULATIONS

To test the performance of the closure models, we use the ARPS code to simulate a neutral boundary layer flow

case similar to that of Andren *et al.* (1994). ARPS was developed and tested at the Center for Analysis and Prediction of Storms at the University of Oklahoma over the last decade. Details on the ARPS code can be found in Xue *et al.* (2001). The equations have been slightly modified to make them closer to the incompressible case studied by Andren *et al.* (1994), as detailed in Xu *et al.* (1996).

The no-slip condition cannot be applied at the bottom boundary in atmospheric boundary layer simulations because the surface is rough. Hence, the top and bottom boundaries are treated as rigid or free-slip boundaries, and surface fluxes are parameterized to account for the influence of the rough bottom surface. The ARPS code parameterizes the momentum fluxes at the surface using a logarithmic drag law (with stability-dependent similarity options).

The flow is driven by a constant geostrophic pressure gradient which would balance a geostrophic wind of $(U_g, V_g) = (10, 0)m/s$. The Coriolis parameter, f , is set equal to 9×10^{-5} . The bottom roughness is set to $0.1m$. At the lateral boundaries, periodic conditions are used for this idealized flat-terrain study. This configuration results in an Ekman-like spiral for the mean velocities. The grid size is $40 \times 40 \times 40$ with grid spacings of $32m \times 32m$ in the horizontal. In the vertical, a stretched grid is used, with $8m$ spacing near the bottom and up to $104m$ near the top of the domain, giving an average spacing of $37.5m$. The anisotropic filter for the modified Clark model was applied at twice the grid spacing, in computational space. Simulations were run for $100000s$ (approximately 10 inertial time periods, tf) with a $0.5s$ large timestep, and $0.05s$ small timestep.

The mean velocity profile is expected to be logarithmic in the lowest region of the boundary layer, as can be shown from similarity theory (Blackadar and Tennekes 1968). As noted by Andren *et al.* (1994), one of the many short-comings of the widely-used eddy viscosity models is their failure to produce logarithmic profiles. Such errors near the wall can affect the entire flow solution. A convenient measure of the model's performance in this respect is the non-dimensional velocity gradient, Φ , which is defined as

$$\Phi = \frac{\kappa z}{u_*} \sqrt{\left(\frac{\partial \langle \bar{u} \rangle}{\partial z}\right)^2 + \left(\frac{\partial \langle \bar{v} \rangle}{\partial z}\right)^2}. \quad (7)$$

Here κ is the von Kármán constant, chosen to be 0.4; u_* is the surface friction velocity defined by $u_* = (\overline{uw}_0^2 + \overline{vw}_0^2)^{1/4}$, where \overline{uw}_0 and \overline{vw}_0 are the total stresses at the lower boundary. For the parameters chosen, u_* is found to be approximately 0.4. In a logarithmic region, $\Phi = 1$, which we expect for approximately the first $200m$ above the wall. Vertical profiles are averaged horizontally in space (denoted by the brackets $\langle \rangle$), as well as in time over the last $20000s$ of the simulation, using data taken at $1000s$ intervals.

Stress profiles for uw are shown in Figure 2 where the contribution of each component in the closure model can be seen. The total stress is approximately linear, as expected in a boundary layer flow. The stress profiles are also shown on a log plot to magnify the region near the wall. The influence of the canopy model decreases as the canopy top is approached, which is selected to be $4 * dx$ ($128m$), or equivalent to the minimum well-resolved horizontal eddy size beneath the filter. We obtain good results when we choose the canopy coefficient C_c so that the canopy model contributes an amount equal to half the wall stress at the first grid point above

the wall. We also apply damping to the canopy model using $(1 - \exp(-z/d))^2$ (with $d = 15m$) very near the wall to slightly reduce the canopy effect there as it was found to be too large. The Smagorinsky coefficient is chosen as $C_s = 0.21$, the standard value used in the ARPS code. The modified Clark term decays to zero naturally at the wall in the presence of the other two model components.

Profiles of Φ are shown in Figure 3. We compare our results with the hybrid closure model to those using the standard Smagorinsky eddy viscosity model. We see that the overshoot in the value of Φ reaches 1.8 for the traditional Smagorinsky model, indicating the model provides excessive shear near the surface. When the modified Clark, canopy, and Smagorinsky models are used together, the overshoot in the value of Φ near the wall from the Smagorinsky model is compensated by the designed tendency for the canopy model to produce Φ values less than unity. In addition, the modified Clark component is of scale-similar form, and thus allows backscatter, or energy flux from the small to the large scales. This is believed to be especially important when the large scales are not fully resolved in the atmospheric boundary layer (Mason and Thomson 1992), and aids in achieving a logarithmic mean velocity profile. Except for at the lowest point, values of Φ within 0.2 of the ideal are obtained using the hybrid model, which represents a significant improvement. With a subset of only one or two components of this hybrid model (e.g., Smagorinsky and series models without the canopy), the results are not as good.

5. CONCLUSIONS

Our conclusion is that the context provided by Carati *et al.* (2001), is useful and leads to insights about model behavior. We are able to achieve improved non-dimensional shear Φ profiles by a systematic use of the models cited above. We have found that when applied to simulations of the atmospheric boundary layer, the SFS series model (Katopodes *et al.* 2000a,b) needs augmentation because of finite grid resolution, and further special treatment at the lower rough boundary. The Smagorinsky model has been used to provide necessary dissipation, without incurring the expected drawbacks of this model as it is used in conjunction with a scale-similarity model. Near the earth's surface, resolution is generally not adequate to resolve many of the turbulent motions and a supplemental model such as the canopy model improves the results. Further work is required for a careful assessment of the canopy model, as a more robust selection process for the coefficients in this model is desired.

6. ACKNOWLEDGMENTS

The support of NSF Grant ATM-0073395 (Physical Meteorology Program: R.R. Rogers, Program Director) is gratefully acknowledged.

7. REFERENCES

- Andren, A., Brown, A.R., Graf, J., Mason, P.J., Moeng, C.-H., Nieuwstadt, F.T.M. and U. Schumann, 1994: Large-eddy simulation of a neutrally stratified boundary layer: A comparison of four computer codes. *Q. J. R. Meteorolo. Soc.*, **120**, 1457.
- Blackadar, A.K. and H. Tennekes, 1968: Asymptotic similarity in neutral barotropic planetary boundary layers. *J. Atmos. Sci.*, **25**, 1015.

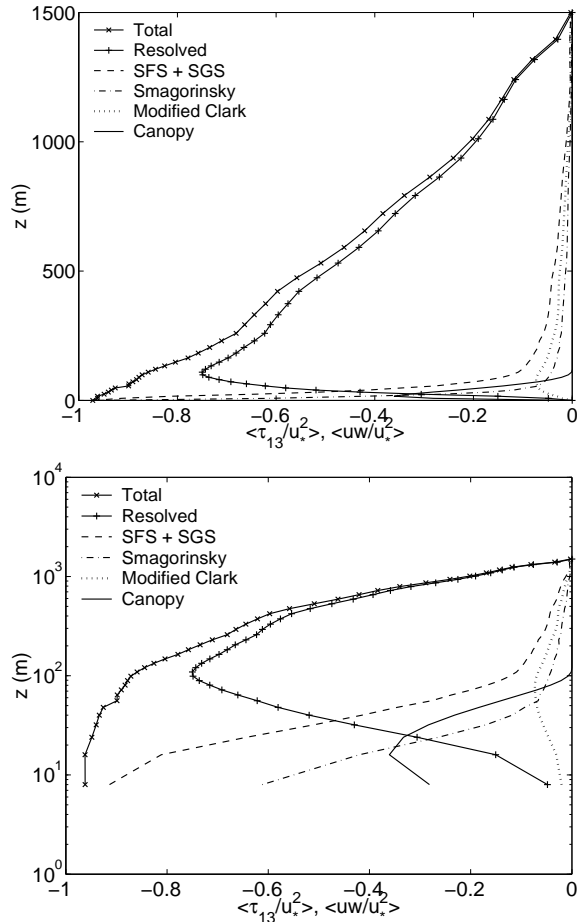


Figure 2: Total stress profiles for uw vertical plane, shown for the hybrid model (modified Clark, Smagorinsky, and canopy), with each model component shown separately in addition to the resolved stress. Profiles have been normalized by u_*^2 . Bottom plot has a logarithmic vertical axis to magnify the region near the wall.

Brown, A.R., Hobson, J.M. and N. Wood, 2001: Large-eddy simulation of neutral turbulent flow over rough sinusoidal ridges. *Boundary-Layer Meteorology*, **98**(3), 411.

Carati, D., Winckelmans, G.S. and H. Jeanmart, 2001: On the modelling of the subgrid-scale and filtered-scale stress tensors in large-eddy simulation. *J. Fluid Mechanics*, **441**, 119.

Cederwall, R.T., 2001: Large-eddy simulation of the evolving stable boundary layer over flat terrain. *Ph.D. Thesis, Stanford University*.

Cederwall, R.T. and R.L. Street, 2002: Investigation of episodic enhancement of turbulence in the stable boundary layer using large-eddy simulation. *15th Symp. on Boundary Layer Turb.*

Chow, F.K. and P. Moin, 2002: A further study of numerical errors in large-eddy simulations. *J. Comp. Phys.*, submitted.

Clark, R.A., Ferziger, J.H. and W.C. Reynolds, 1977: Evaluation of subgrid-scale turbulence models using a fully simulated turbulent flow. *Technical Report TF-9, Department of Mechanical Engineering, Stanford University*.

Domaradzki, J.A. and E.M. Saiki, 1997: A subgrid-scale model based on the estimation of unresolved scales of turbulence. *Phys. Fluids*, **9**(7), 2148.

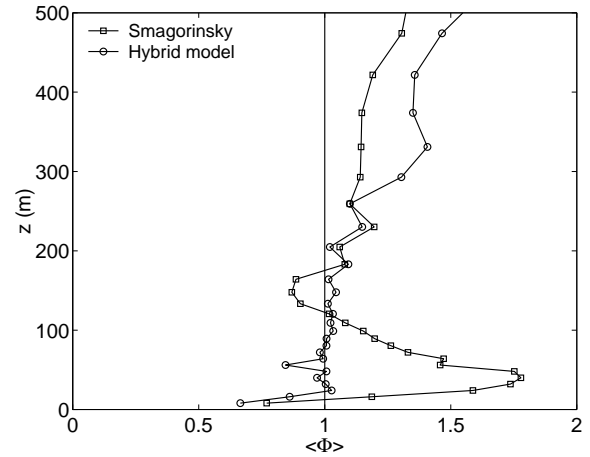


Figure 3: Comparison of non-dimensional mean shear Φ profiles for the Smagorinsky model and for the hybrid model (modified Clark, Smagorinsky, and canopy).

Fischer, P. and T. Iliescu, 2001: A 3D channel flow simulation at $Re_\tau = 180$ using a rational LES model. *Third AFOSR International Conference on DNS/LES*, 283.

Geurts, B.J., 1997: Inverse modeling for large-eddy simulation. *Phys. Fluids*, **9**(12), 3585.

Ghosal, S., 1996: An analysis of numerical errors in large-eddy simulations of turbulence. *J. Comp. Phys.*, **125**, 187.

Hughes, T.J.R., Mazzei L., Oberai A.A., and A.A. Wray, 2001: The multiscale formulation of large eddy simulation: Decay of homogeneous isotropic turbulence. *Phys. Fluids*, **13**(2), 505.

Katopodes, F.V., Street, R.L. and J.H. Ferziger, 2000a: A theory for the subfilter-scale model in large-eddy simulation. *Technical Report 2000-K1, Environmental Fluid Mechanics Laboratory, Stanford University*.

Katopodes, F.V., Street, R.L. and J.H. Ferziger, 2000b: Subfilter-scale scalar transport for large-eddy simulation. *14th Symp. on Boundary Layer Turb.*, 472.

Mason, P.J. and D.J. Thomson, 1992: Stochastic backscatter in large-eddy simulations of boundary layers. *J. Fluid Mech.*, **242**, 51.

Smagorinsky, J., 1963: General circulation experiments with the primitive equations. *Mon. Weather Rev.*, **93**, 99.

Stolz, S. and N.A. Adams, 1999: An approximate deconvolution procedure for large-eddy simulation. *Phys. Fluids*, **11**(7), 1699.

van Dijk, A. and P. Duynkerke, 2002: The role of the filter in the filtered Navier-Stokes equation. *Phys. Fluids*, submitted.

Vreman, B., Geurts, B. and H. Kuerten, 1996: Large-eddy simulation of the temporal mixing layer using the Clark model. *Theoretical and Computational Fluid Dynamics*, **8**, 309.

Winckelmans, G.S., Wray, A.A., Vasilyev, O.V. and H. Jeanmart, 2001: Explicit-filtering large-eddy simulation using the tensor-diffusivity model supplemented by a dynamic Smagorinsky term. *Phys. Fluids*, **13**(5), 1385.

Xu, Q., Xue, M. and K.K. Droegemeier, 1996: Numerical simulations of density currents in sheared environments within a vertically confined channel. *J. Atmos. Sci.*, **53**(5), 770.

Xue, M., Droegemeier, K.K. and V. Wong, 2001: The Advanced Regional Prediction System (ARPS) : A multi-scale non-hydrostatic atmospheric simulation and prediction model. Part I: Model dynamics and verification. *Meteorology and Atmospheric Physics*, **75**(3-4), 161.

Zang, Y., Street, R.L. and J.R. Koseff, 1993: A dynamic mixed subgrid-scale model and its application to turbulent recirculating flows. *Phys. Fluids A*, **5**(12), 3186.

Zhou, Y., Brasseur, J.G. and A. Juneja, 2001: A resolvable subfilter-scale model specific to large-eddy simulation of under-resolved turbulence. *Phys. Fluids*, **13**(9), 2602.